Applied Microbiology and Biotechnology
https://doi.org/10.1007/s00253-020-10616-w

APPLIED MICROBIAL AND CELL PHYSIOLOGY

Plasmid expression level heterogeneity monitoring via heterologous eGFP production at the single-cell level in *Cupriavidus necator*

Catherine Boy[1] · Julie Lesage[1] · Sandrine Alfenore[1] · Nathalie Gorret[1] · Stéphane E. Guillouet[1]

Received: 28 January 2020 / Revised: 2 April 2020 / Accepted: 6 April 2020
© Springer-Verlag GmbH Germany, part of Springer Nature 2020

Abstract

A methodology for plasmid expression level monitoring of eGFP expression suitable for dynamic processes was assessed during fermentation. This technique was based on the expression of a fluorescent biosensor (eGFP) encoded on a recombinant plasmid coupled to single-cell analysis. Fluorescence intensity at single-cell level was measured by flow cytometry. We demonstrated that promoter evaluation based on single-cell analysis versus classic global analysis brings valuable insights. Single-cell analysis pointed out the fact that intrinsic fluorescence increased with the strength of the promoter up to a threshold. Beyond that, cell permeability increases to excrete the fluorescent protein in the medium. The metabolic load due to the increase in the eGFP production in the case of strong constitutive promoters leads to slower growth kinetics compared with plasmid-free cells. With the strain *Cupriavidus necator* Re2133, growth rate losses were measured from 3% with the weak constitutive promoter P_{lac} to 56% with the strong constitutive promoter P_{j5}. Through this work, it seems crucial to find a compromise between the fluorescence intensity in single cells and the metabolic load; in our conditions, the best compromise found was the weak promoter P_{lac}. The plasmid expression level monitoring method was tested in the presence of a heterogeneous population induced by plasmid-curing methods. For all the identified subpopulations, the plasmid expression level heterogeneity was significantly detected at the level of fluorescence intensity in single cells. After cell sorting, growth rate and cultivability were assessed for each subpopulation. In conclusion, this eGFP biosensor makes it possible to follow the variations in the level of plasmid expression under conditions of population heterogeneity.

Key Points

- *Development of a plasmid expression level monitoring method at the single-cell level by flow cytometry.*
- *Promoter evaluation by single-cell analysis: cell heterogeneity and strain robustness.*
- *Reporter system optimization for efficient subpopulation detection in pure cultures.*

Keywords Plasmid stability · Expression level · Biosensor · Flow cytometry · Cell sorting · *Cupriavidus necator* H16

Introduction

Microbial populations grown in supposedly homogeneous environments are often still considered as being composed of identical individuals. Several studies have proven the opposite even in the case of cultures derived from monoclonal colonies (Carlquist et al. 2012; Delvigne and Goffin 2014; Muller et al. 2010; Zielenkiewicz and Ceglowski 2001). Subpopulation heterogeneities can be divided into four main categories: genetic, biochemical, physiological, and phenotypic (Brehm-Stecher and Johnson 2004). There are often connections between these categories (Martins and Locke 2015). Genetic heterogeneity can be caused by spontaneous point mutations, transcription errors, or mobile genetic elements (Brehm-Stecher and Johnson 2004; Elowitz et al. 2002; Martins and Locke 2015). Biochemical heterogeneity is defined by differences in macromolecular composition (Martins and Locke 2015) or activity levels. It can be caused by genetic heterogeneity and variations in cell cycle–related processes (Brehm-Stecher and Johnson 2004; Martins and Locke 2015). Physiological heterogeneity shows morphological

Electronic supplementary material The online version of this article (https://doi.org/10.1007/s00253-020-10616-w) contains supplementary material, which is available to authorized users.

✉ Nathalie Gorret
ngorret@insa-toulouse.fr

[1] TBI, Université de Toulouse, CNRS, INRAE, INSA, Toulouse, France

heterogeneities between cell subpopulations. It can be explained by antibiotic presence or by nutrient availability, and also by variations in the cell cycle. Phenotypic heterogeneity is defined as the consequence of genetic, biochemical, and/or physiological heterogeneities (Brehm-Stecher and Johnson 2004).

In large-scale bioreactors, population heterogeneity is presumed to reduce production yields and increase process instability. So, ensuring phenotypic homogeneity of engineered microbial populations is of major interest for synthetic biology and bioprocess optimization (Binder et al. 2017).

On the one hand, phenotypic variation between clonal populations is a natural phenomenon that arises from stochastic gene expression and/or fluctuations in the cell cycle. Therefore, this noise in the phenotypic behavior of the cell can originate from the biochemical process of gene expression itself (Elowitz et al. 2002; Mortier et al. 2019; Nana et al. 2018).

On the other hand, maintenance and expression of heterologous genes add a metabolic burden on host cells. Some of these metabolic burdens are due to specific roles of the recombinant genes in the engineered strains (e.g., metabolite consumption by a heterologous enzyme). However, the majority of metabolic burdens observed are due to the consumption of cellular transcriptional resources during recombinant gene expression (Ceroni et al. 2018). So, two major biological mechanisms are competing within engineered strains: recombinant gene maintenance and cell growth (Silva et al. 2012). In this context, this resource reassignment will have a major impact on translation, especially if numerous mRNA expressed from the recombinant sequence encode for strong RBS (i.e., ribosome binding sites) sequences and require an increased number of ribosomes that will no longer be available for the host gene expression. Metabolic burden due to recombinant molecule expression has a stronger impact at the level of protein translation. The consequences of metabolic load are often a decrease of the growth rate and global physiological modifications, all of this leading to a decrease in the engineered microorganism performances toward the production of the recombinant molecule (Ceroni et al. 2018).

Numerous expression systems are based on plasmid vectors for recombinant molecule production, both in research and industry. However, many cases of expression instability have been reported and the causes are still often misunderstood. First, plasmid replication frequency must be high enough to ensure equal partition between daughter cells, but also reasonable to prevent host cell exhaustion because of plasmid-induced metabolic load (Wegrzyn and Wegrzyn 2002). The relative importance of metabolic load due to recombinant protein production depends on various parameters like the amount of protein produced, plasmid copy number and size, host cell metabolic state, or growth medium composition (Bentley and Quiroga 1993; Glick 1995). Then, plasmid partitioning should be efficiently performed between daughter cells. Finally, because of their decreased metabolic load, plasmid-less cells have a higher growth rate than plasmid-bearing cells; the resulting growth rate difference intensifies segregational instability (Bentley et al. 1990; De Gelder et al. 2007).

Various tools have been developed to study population heterogeneity in single cells regarding expression level heterogeneity, like single-cell RT-PCR and RNA-seq or FISH (fluorescence in situ hybridization) (Haroon et al. 2013; Lee et al. 2006; Loftie-Eaton et al. 2014; Skulj et al. 2008; Tal and Paulsson 2012). Nevertheless, most of them are time consuming and not adapted to the constraints of fermentation processes which require a suitable monitoring method under dynamic conditions. Plus, they were designed on eukaryotic cells and will require further development to be suitable to smaller cells like prokaryotes (Gonzalez-Cabaleiro et al. 2017).

Cupriavidus necator H16 is a chemolithoautotrophic Gram-negative bacterium which belongs to the beta-subclass of *Proteobacteria*. *C. necator* has a versatile metabolism and is naturally able to consume oils (Budde et al. 2011), carboxylic acids (Friedrich et al. 1979; Grunwald et al. 2015; Johnson 1971), carbohydrates (Grousseau et al. 2014; Johnson 1971), and carbon dioxide (Crepin et al. 2016; Marc et al. 2017). Lately, *C. necator* has been engineered as a bioproduction platform for the biosynthesis of alcohols (Gruber et al. 2014; Marc et al. 2017), alka(e)ne (Crepin et al. 2016), carboxylic acids (Ewering et al. 2006; Hoefel et al. 2010), and methyl ketones (Muller et al. 2013). Two main strategies for the introduction of heterologous genes in *C. necator* have been developed: plasmids (Bi et al. 2013; Grousseau et al. 2014; Gruber et al. 2014, 2015, 2016; Sato et al. 2013; Sydow et al. 2017) and chromosomal insertion (Budde et al. 2011; Mifune et al. 2010; Wong et al. 2012). Developing and improving tools for the molecular engineering of *C. necator* H16 would open up to new possibilities in terms of synthetic biology of the strain.

Our aim consisted in being able to monitor expression heterogeneity throughout fermentation processes as efficiently and accurately as possible. So, it was necessary to develop a fast and reliable method to follow the expression of plasmid-encoded genes under dynamic conditions. The favored methodology was the expression of a plasmid-encoded reporter protein: enhanced green fluorescent protein (eGFP) (Cinelli et al. 2000; Shaner et al. 2005). This approach allows the use of flow cytometry, which has been reviewed in many studies as being a relevant method to monitor single-cell variability under dynamic conditions (Delvigne and Goffin 2014; Muller and Nebe-von-Caron 2010; Tracy et al. 2010). The first objective was to characterize a constitutive promoter driving *egfp* expression with the lowest impact as possible on host metabolism in terms of growth and physiology. The second objective was to ensure significant single-cell fluorescence

intensity levels. Consequently, a compromise needed to be reached between these two issues. The work was supported by kinetic data and viability measurements to determine the most suitable constitutive promoter to induce eGFP production within the framework of plasmid stability monitoring. The third objective was to verify that our plasmid expression level biosensor successfully allowed monitoring expression heterogeneity in experimental conditions where population heterogeneity had been induced artificially. For that purpose, the designed strain bearing the plasmid encoding for the expression level reporter was exposed to plasmid-curing-like conditions.

Material and methods

Strains, plasmids, and media

Strains

C. necator Re2133 (Budde et al. 2011) was used as expression strain. This strain was obtained by deleting genes encoding for acetoacetyl-CoA reductases (*phaB1B2B3*) and for PHA synthase (*phaC1*) from the wild-type strain *C. necator* H16/ATCC17699 which was gentamicin resistant (Gen^R). The strains *Escherichia coli* S17-1 and Top10 were used during plasmid construction.

Media

The rich medium for precultures was composed of 27.5 g·L^{-1} tryptic soy broth (TSB, Becton Dickinson, Sparks, MD, USA) with addition of 10 mg·L^{-1} gentamicin and 200 mg·L^{-1} kanamycin as final concentration. For tryptic soy agar (abbr. TSA) plates, 20 g·L^{-1} agar was added to the TSB medium.

For molecular biology, the rich lysogeny broth (abbr. LB) medium was used and composed of 10 g·L^{-1} of peptone, 5 g·L^{-1} of yeast extract, and 10 g·L^{-1} of NaCl (i.e., sodium chloride). For LB agar plates, 20 g·L^{-1} agar was added to the LB medium.

The mineral medium used for flask cultivation was previously described in Lu et al. (2013). Gentamicin (10 mg·L^{-1}) and kanamycin (200 mg·L^{-1}) were added to this medium. Fructose (20 g·L^{-1}) and NH_4Cl (0.5 g·L^{-1}) were respectively used as carbon and nitrogen sources. The mineral medium used for bioreactor cultivation was previously described in Marc et al. (2017). Fructose (50 g·L^{-1}) was used as carbon source.

Plasmids

The plasmids used in this work are enlisted in Table 1. The design of the pKRSF1010 plasmids was detailed in Gruber et al. (2014). The plasmid pCB1 was designed and constructed in the team. The plasmid backbone pBBad (Fukui et al. 2009, 2011) was chosen; pBBad had previously been used in our team for the construction of *C. necator* recombinant strains toward the production of heterologous molecules of interest.

The sequence of interest P_{lac}-egfp was amplified from the plasmid pKRSF1010-P_{lac}-egfp using the forward primer pBBAD_Plac_acl1_fw and the reverse primer pBBAD_egfp_acl1_rv listed in Supplementary Data 1. Primers were obtained from Eurogentec (Angers, France). DNA sequence amplification was achieved using Phusion High-Fidelity PCR Master Mix with GC Buffer (New England Biolabs, France) and led on the Mx3005P QPCR System (Agilent Technologies, USA). PCR products were purified with the Monarch® PCR & DNA Cleanup Kit (New England Biolabs, USA).

The plasmid pBBad was linearized by the restriction enzyme *AclI* (New England Biolabs, USA) using NEB protocol recommendations and then purified by gel agarose extraction with the QIAquick gel extraction kit of Qiagen ® (Qiagen, Germany).

The cloning of the P_{lac}-egfp cassette into the plasmid vector pBBad was achieved through Gibson Isothermal Assembly®. The insert to vector ratio applied was 10:1 (w:w). Reaction took place at 50 °C for 30 min. Assembly products were transformed into high-efficiency *E. coli* Top 10 (Invitrogen, USA) chemical competent cells by heat shock. After growth, green colonies of *E. coli* Top10 were selected for plasmid purification with the QIAprep Spin Miniprep Kit (Qiagen, Germany). Screen PCR with OneTaq Hot Start 2X Master Mix with GC Buffer (New England Biolabs, USA) was used to verify the correct gene insertion. Plasmid constructions were confirmed by sequencing. Then, all constructed plasmids were transformed into electrocompetent *E. coli* S17-1 (ATCC 47055) by electroporation like that described in Crépin et al. (Crepin et al. 2016). Finally, conjugative transfer of plasmids from *E. coli* S17-1 to *C. necator* Re2133 was achieved like that in Slater et al. (1998).

Precultures and flask cultivations on fructose

One glycerol stock was plated on TSA plates (tryptic soy agar, TSB with 20 g·L^{-1} agar) containing 10 mg·L^{-1} gentamicin and 200 mg·L^{-1} kanamycin. The plates were incubated for 72 h at 30 °C. One colony was used to inoculate a rich medium flask culture (3 mL), which was grown for 48 h at 30 °C and 110 rpm. Then, the whole broth volume was used to inoculate a 30-mL mineral medium culture flask, which was incubated at 30 °C and 110 rpm for 24 h. Finally, the whole broth volume was used to inoculate a 300-mL mineral medium culture flask. The baffled flasks were incubated at 30 °C and 110 rpm for 10 h. Broth samples were taken regularly during this step.

Table 1 List and characteristics of the plasmids used in this work

Plasmid	Description	Reference
pKRSF1010-P_{lac}-eGFP	Kan^R, P_{lac}, egfp, par, RSF1010 mob, and oriV	(Gruber et al. 2014)
pKRSF1010-P_{tac}-eGFP	Kan^R, P_{tac}, egfp, par, RSF1010 mob, and oriV	(Gruber et al. 2014)
pKRSF1010-P_{n25}-eGFP	Kan^R, P_{n25}, egfp, par, RSF1010 mob, and oriV	(Gruber et al. 2014)
pKRSF1010-P_{j5}-eGFP	Kan^R, P_{j5}, egfp, par, RSF1010 mob, and oriV	(Gruber et al. 2014)
pBBad	Kan^R; PBad; pBBR1MCS-2 derivative	(Fukui et al. 2009)
pCB1	Kan^R, P_{lac}-eGFP; PBad; pBBR1MCS-2 derivative	This work

Batch cultivations on fructose

Batch cultivations consisted in non-limited growth on fructose. The cultures were led in a 5-L bioreactor Biostat®B-DCU (Sartorius, Germany) with a working volume of 3 L. Regulation and monitoring were done using MFCS/win 2.1 software package (Sartorius, Germany). Partial pressure of dioxygen (pO_2) in the medium was measured with the optical oxygen sensor InPro 6860i (Mettler Toledo, USA) and pH value was measured with a pressurized gel-filled pH electrode (Mettler Toledo, USA).

Temperature was regulated at 30 °C and pH level at 7.0 by addition of a 4 M KOH solution. Fermentation was carried out in aerobic conditions (i.e., air flow and stirring rates were regulated to maintain pO_2 above 30%). The initial fructose concentration in the medium was 50 $g{\cdot}L^{-1}$. To prevent nutrient limitation, pulses of rich phosphate solution (7 $mL{\cdot}L^{-1}$) and trace element solution (2 $mL{\cdot}L^{-1}$) were carried out every 10 $g{\cdot}L^{-1}$ of biomass produced.

Plasmid-curing subcultures

One glycerol stock was plated on a TSA plate with addition of 10 $mg{\cdot}L^{-1}$ gentamicin and 200 $mg{\cdot}L^{-1}$ kanamycin. The plate was incubated for 72 h at 30 °C. A single colony was used to inoculate 10 mL TSB with 10 $mg{\cdot}L^{-1}$ gentamicin and 200 $mg{\cdot}L^{-1}$ kanamycin in a flask. The flasks were incubated 24 h at 30 °C and 110 rpm. Then, this culture was used to inoculate 30 mL of flask mineral medium with 10 $mg{\cdot}L^{-1}$ gentamicin and 200 $mg{\cdot}L^{-1}$ kanamycin at 0.1 $g{\cdot}L^{-1}$of biomass. This step was considered as the positive control for reference fluorescence intensity distribution. The next subcultures, and all the others that followed, were started by a tenfold dilution in flask mineral medium without any antibiotics and grown at 37 °C and 110 rpm until a concentration of 1 $g{\cdot}L^{-1}$ biomass was reached. At every subculture starting point and endpoint, the optical density (600 nm) was measured and the samples were analyzed by flow cytometry.

Analytical procedure

Biomass characterization

Biomass growth was monitored by measuring optical density (OD) at 600 nm using a visible spectrophotometer (DR3900, Hachlange, Loveland, CO, USA) with a 0.2-cm path length absorption cell (Hellma). OD was calibrated against cell dry weight (CDW) measurements: 2 $g_{CDW}{\cdot}L^{-1}$ corresponds to 1 OD unit. Beforehand, 0.2-μm pore-size polyamide membranes (Sartorius, Göttingen, Germany) were dried to a constant weight at 60 °C under partial vacuum (200 mmHg) in an oven (HERAEUS, France) for 72 h and weighted. For dry weight measurements, culture medium was harvested and filtrated on the before-mentioned membranes which were then dried again to a constant weight at 60 °C under partial vacuum (200 mmHg) for 72 h.

Plate count

Plate count method was based on the ability of plasmid-bearing cells to grow on a selective medium. In our case, *C. necator* is naturally resistant to gentamycin. Kanamycin resistance is encoded on all plasmids. As a result, we consider that *C. necator* plasmid–bearing cells are those able to grow under the double antibiotic selective pressure.

Two series of plates were used: TSA with only 10 $mg{\cdot}L^{-1}$ gentamicin and TSA with both 10 $mg{\cdot}L^{-1}$ gentamicin and 200 $mg{\cdot}L^{-1}$ kanamycin. Serial dilutions were carried out in 9-mL physiological water (0.85% NaCl) tubes (BioMérieux, Marcy-l'Étoile, France). For every sample, three different dilutions were tested depending on the biomass concentration (generally between 10^{-5} and 10^{-9}). One hundred microliters of the diluted sample was plated in triplicate using the Whitley Automated Spiral Plater (WASP, Don Whitley Scientific, Shipley, UK).

Flow cytometry

eGFP fluorescence and cell viability were monitored with a BD Accuri C6® flow cytometer (BD Biosciences, Franklin

Lakes, NJ, USA). The device is equipped with blue (488 nm) and red (640 nm) excitation lasers. Light scatter is collected from two angles: forward (FSC, 0° ± 13) and side (SSC, 90° ± 13) scatter. Fluorescence intensity is measured by four detectors: FL1 (533 ± 30 nm), FL2 (585 ± 40 nm), FL3 (> 670 nm), and FL4 (675 ± 25 nm).

Propidium iodide (PI, Molecular Probes, Invitrogen, USA) was used to evaluate membrane permeability as a cell viability indicator. Commercial solution is composed of 20 mM PI in anhydrous dimethyl sulfoxide (*abbr.* DMSO) solvent and was diluted at a concentration of 20 μM before use. First, culture samples were diluted in 0.9% NaCl to reach approximately a cell concentration of 10^6 cells mL^{-1}. Then, the cells were stained by 20 μL of PI working solution and incubated for 20 min at room temperature in the dark. A 100% dead-cell control was prepared by incubating cells in 70% isopropanol for 1 h at room temperature.

Sample runs were performed (until 20,000 events were counted) at the slow flow rate setting (14 μL $\cdot min^{-1}$) using milli-Q water as sheath fluid. The FSC signal (threshold, 12,000) and SSC signal (threshold, 2000) were used as trigger channels.

Green fluorescence of eGFP was collected in the FL1 channel and red fluorescence of PI in the FL3 channel. Data acquisition was performed with BD Accuri CFlow® software. Data processing was achieved with FlowJo software (Becton Dickinson, Sparks, MD, USA).

Fluorescence measurement in the medium

Broth samples were centrifuged for 3 min at 13,000 rpm with a MiniSpin® table-top microcentrifuge (Eppendorf, Germany) and supernatants were used for fluorescence measurement.

Fluorescence unit measurements were achieved with the Synergy™ HT (Biotek®, USA) at excitation wavelength of 485 ± 20 nm and emission wavelength of 525 ± 20 nm. The sensitivity of the device was set at 50. Black Nunclon® 96-well plates (Thermo Fisher, USA) were used.

Fluorescence-activated cell sorting

Cell sorting experiments were led on the MoFlo Astrios EQ cell sorter using the Summit v6.3 software (Beckman Coulter, USA). Cell sorting was conducted with a 70-μm nozzle and 60-psi operating pressure. The sorting speed was set around 30,000 events per second. The single-cell mode for the sort mode and 0.5 drop for the droplet envelope were chosen. Cell samples were diluted in 0.9% NaCl prior to the sorting experiment.

Based on the FSC-Area vs SSC-Area (488 nm laser) plot and the FSC-Height vs FSC-Area (488-nm laser) plot, single cells with similar cell size and granularity were first selected. Then, based on the histogram of the eGFP fluorescence (488-nm laser, 526/52 filter), single cells were sorted depending on their fluorescence intensity.

Black and transparent Nunclon® 96-well plates (Thermo Fisher, USA) were used. Every single cell was dropped in a well from a 96-well plate. For each cell subpopulation, a total amount of six 96-well plates was generated. Two series of two 96-well plates were generated for each subpopulation: one set in transparent plates and one set in black plates; one plate of each serial contained TSB + 5 $mg \cdot L^{-1}$ gentamicin and one plate of each serial contained TSB + 5 $mg \cdot L^{-1}$ gentamicin + 50 $mg \cdot L^{-1}$ kanamycin. For every subpopulation, two transparent 96-well plates were generated to evaluate growth on solid medium. One plate contained TSA + 5 $mg \cdot L^{-1}$ gentamicin and one with TSA + 5 $mg \cdot L^{-1}$ gentamicin + 50 $mg \cdot L^{-1}$ kanamycin.

The TSB liquid plates were incubated at 30 °C and 40 rpm. Measurements of optical density and fluorescence unit were achieved every 8 h. For every TSB liquid plate, when the exponential phase was reached and around 7 cell generations, the fluorescence intensity distribution was determined in every well by flow cytometry.

The TSA solid plates were incubated at 30 °C and after growth, CFU was counted and observed under blue light with a blue light transilluminator (Thermo Fisher, USA) to reveal green fluorescent colonies.

Statistical analysis: Normality of distribution functions by boxplot representation

Boxplots are graphical tools used to represent an empirical distribution through some simple localization parameters: the median (50th percentile, red line), the first quartile (25th percentile), and the third quartile (75th percentile). The first and third quartiles respectively represent the bottom and top of the boxplot (Fig. 1d). The median, or second quartile, was represented by the line inside the box. The interquartile range (IQR) was situated between the first and third quartiles and represents the length of the box. The whiskers represent the minimum and maximum values when they are within 1.5 × IQR from both extremities of the box. Values above 1.5 × IQR were considered as outliers and are represented by points. A symmetric boxplot with its median in the middle of the box and same length whiskers might be expected to be normally distributed (Rakotomalala 2011).

Results

Our aim was to develop a quick and reliable plasmid expression level monitoring technique suitable for

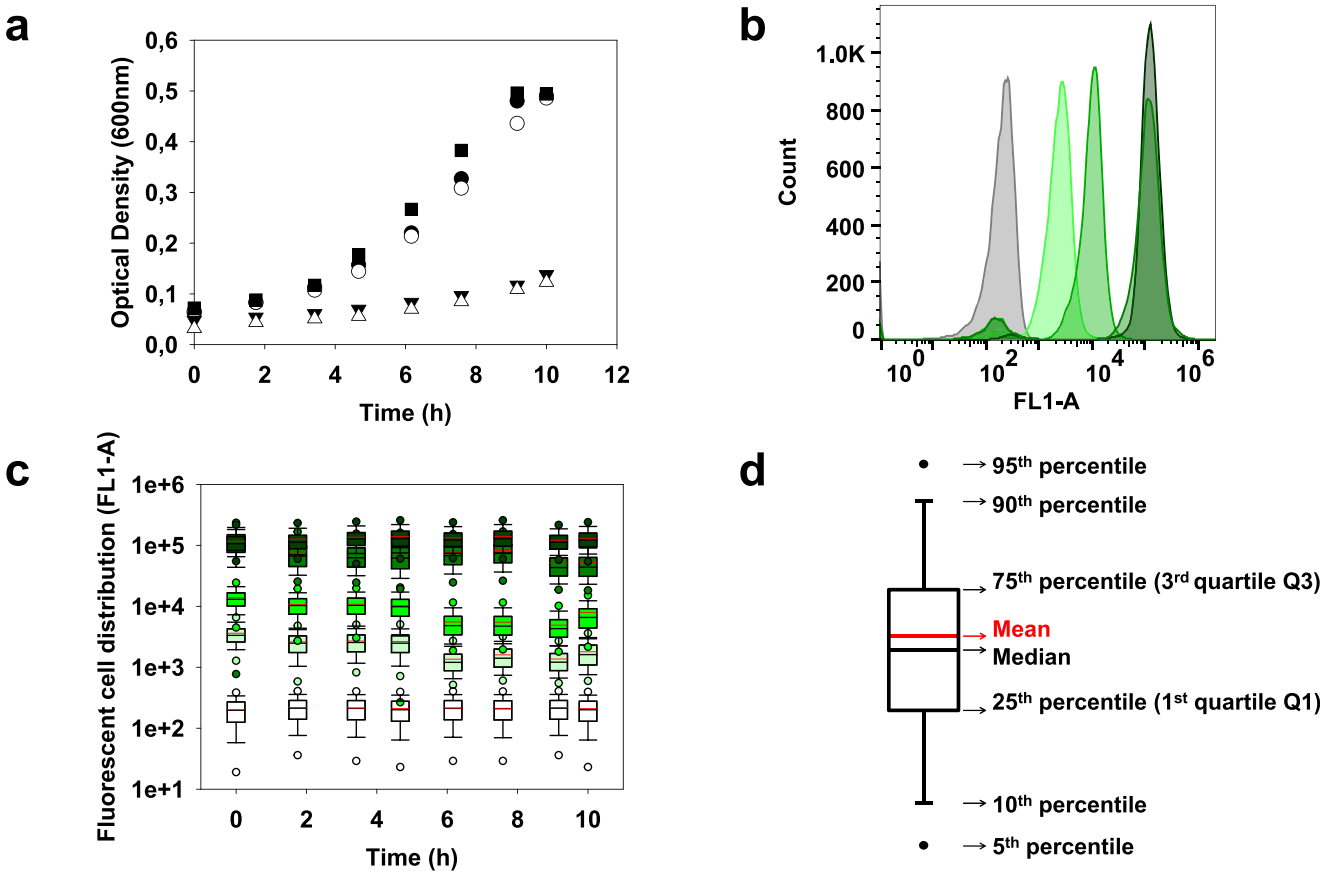

Fig. 1 **a** Growth kinetic in flasks of *Cupriavidus necator* Re2133 strains, harboring plasmids encoding for eGFP production with different constitutive promoters: Re2133/pKRSF1010-P_{j5}-eGFP (white-filled up-pointing triangle), Re2133/pKRSF1010-P_{n25}-eGFP (black-filled down-pointing triangle), Re2133/pKRSF1010-P_{tac}-eGFP (white-filled circle), Re2133/pKRSF1010-P_{lac}-eGFP (black-filled circle), and Re2133 (black-filled square). Data obtained by optical density measurements at 600 nm. **b** Fluorescence intensity distribution of *Cupriavidus necator* Re2133 strains bearing different plasmids based on various promoters. Gray: *C. necator* Re2133; from light to darker shades of green: *C. necator* Re2133 pKRSF1010-P_{lac}-egfp, pKRSF1010-P_{tac}-egfp, pKRSF1010-P_{n25}-egfp, and pKRSF1010-P_{j5}-egfp. Data obtained by flow cytometry in FL1 channel. **c** Boxplot comparing the fluorescence intensity distribution of the different *Cupriavidus necator* Re2133 strains, harboring plasmids encoding for eGFP production with different constitutive promoters (Re2133/pKRSF1010-P_{lac}-egfp, pKRSF1010-P_{tac}-egfp, pKRSF1010-P_{n25}-egfp, pKRSF1010-P_{j5}-egfp) during growth. White: *C. necator* Re2133; from light to darker shades of green: *C. necator* Re2133 pKRSF1010-P_{lac}-egfp, pKRSF1010-P_{tac}-egfp, and pKRSF1010-P_{n25}-egfp. Data obtained by flow cytometry in FL1 channel. **d** Definition of boxplot representation: The boundary of the box closest to zero indicates the 25th percentile, a black line within the box marks the median, a red line within the box marks the mean, and the boundary of the box farthest from zero indicates the 75th percentile. Whiskers above and below the box indicate the 90th and 10th percentiles. The black dot indicates the 95th and 5th percentiles

fermentation processes; this technique was based on the constitutive expression of the recombinant biosensor eGFP by plasmid-bearing cells. Flow cytometry was used as a fast, sensitive, statistically reliable method for fluorescence intensity measurements at the single-cell level which could be implemented for bioreactor on-line monitoring (Bahl et al. 2004). Four constitutive promoters inducing eGFP expression of increasing strength, respectively, P_{lac}, P_{tac}, P_{n25}, and P_{j5}, were evaluated regarding their impact on host cell physiology.

C. necator Re2133 was used as reference strain due to its increasing interest as a cell factory for different biomolecule production, like isopropanol and alkane (Crepin et al. 2016; Grousseau et al. 2014; Marc et al. 2017) under heterotrophic and autotrophic conditions.

Impact of the strength of promoters inducing eGFP production on *C. necator* physiology in flask cultures

Erlenmeyer flask cultures on mineral medium were carried out with *C. necator* Re2133 strains bearing plasmids encoding for eGFP production under the control of P_{j5}, P_{n25}, P_{tac}, and P_{lac} constitutive promoters. These promoters were designed by Gruber et al. (2014) and their strength was measured at the whole population level (Gruber et al. 2014). The plasmid-free strain *C. necator* Re2133 was used as reference.

Impact on growth kinetics

As expected, the growth rate of the plasmid-free strain *C. necator* Re2133 was the highest at $0.26 \pm 0.01\ h^{-1}$ (Fig. 1a). The highest maximum growth rate among plasmid-bearing strains Re2133/pKRSF1010-P_{lac}-egfp and *C. necator* Re2133/pKRSF1010-P_{tac}-egfp was $0.25 \pm 0.01\ h^{-1}$, corresponding to a non-significant loss of 3% compared with the plasmid-free strain. The lowest maximum growth rates were reached by Re2133/pKRSF1010-P_{n25}-egfp and Re2133/pKRSF1010-P_{j5}-egfp with $0.12 \pm 0.01\ h^{-1}$ and $0.11 \pm 0.01\ h^{-1}$, respectively, corresponding to a loss of about 56% and 54% compared with the reference strain.

Fluorescence intensity at the single-cell level

Samples from flask cultures were analyzed by flow cytometry to determine fluorescence intensity distribution at the single-cell level within the whole population. As expected, *C. necator* Re2133 plasmid–free cells do not fluoresce in the FL1-A detection channel of the flow cytometer (Fig. 1b, c). All cells presenting fluorescence intensity above a threshold of 8×10^2 in the FL1-A channel were considered eGFP-positive based on fluorescence intensity of the reference strain Re2133.

All fluorescence intensity distributions presented a normal distribution according to boxplot representation and did not vary during growth (Fig. 1c, d); the means and medians were equal and the whiskers were symmetric compared with the median. Promoter strength can be established by ranking plasmid-bearing strains from lowest to highest fluorescence intensity distribution at the single-cell level (Fig. 1b, c): P_{lac}, P_{tac}, P_{n25}, and P_{j5}. The increase in fluorescence intensity was equal to a half decade between P_{lac} and P_{tac}, one decade between P_{tac} and P_{n25}, and a tenth of a decade between P_{n25} and P_{j5}. No significant differences were observed between the promoters P_{n25} and P_{j5}, reaching the maximum of fluorescent protein accumulation in the cell.

Cell permeabilization and eGFP excretion

Membrane permeability and extracellular fluorescence intensity were evaluated during flask cultures. The impact of the metabolic burden due to different levels of eGFP production was also evaluated through cell permeability. At inoculation, the percentage of permeabilization was low under 5% for P_{lac}, P_{tac}, and P_{n25} but up to 25% for P_{j5}. For P_{lac}, P_{tac}, and P_{n25} promoters, the percentage of PI-positive cells (i.e., propidium iodide–stained cells) increased over time to reach up to 15% for P_{lac}, 13% for P_{tac}, and 22% for P_{n25} whereas for P_{j5}, the percentage did not vary (25%) (Fig. 2a).

The strain Re2133/pKRSF1010-P_{lac}-egfp maintained the lowest extracellular fluorescence intensity over time (Fig. 2b). The same kinetic was observed for pKRSF1010-P_{tac}-egfp except for the last point, which was significantly higher. The strains Re2133/pKRSF1010-P_{n25}-egfp and Re2133/pKRSF1010-P_{j5}-egfp presented with the highest extracellular fluorescence intensity levels. Even for the medium-strength promoter P_{n25}, there was a notable increase in eGFP excretion in the medium.

Although the relative amount of permeabilized cells was equal for Re2133/pKRSF1010-P_{lac}-egfp and Re2133/pKRSF1010-P_{tac}-egfp, the extracellular fluorescence intensity for the promoter P_{tac} was higher than that for P_{lac}. Increased permeabilization percentages for stronger constitutive promoters led to higher extracellular fluorescence intensity.

Plasmid monitoring during batch cultures in the bioreactor

A scale up from flask cultures to 5-L bioreactors was carried out to increase the number of cell generations and to amplify the phenomena described above. Therefore, the impact of the eGFP expression on *C. necator* physiology was further investigated for the two extreme plasmid constructions detailed above: pKRSF1010-P_{lac}-egfp and pKRSF1010-P_{j5}-egfp.

Impact of promoter strength on the growth kinetics

Re2133/pKRSF1010-P_{lac}-egfp reached a mean specific growth rate of $0.23 \pm 0.01\ h^{-1}$ as obtained previously in flasks (Fig. 3a). The Re2133/ pKRSF1010-P_{j5}-egfp strain reached a mean growth rate of $0.13 \pm 0.01\ h^{-1}$. This value was slightly higher than the results obtained in flasks, likely due to a better control of cell environment (i.e., pH regulation, dissolved O_2 level). However, this growth rate could not be maintained for P_{j5} and decreased from 25 h until the end of the culture.

Impact of promoter strength on the fluorescence intensity distribution

For Re2133/pKRSF1010-P_{lac}-egfp, according to the boxplot representation, the fluorescent cell population presented all along the culture, a Gaussian distribution that did not vary (Fig. 3b); means and medians were equal and the boxes as well as the whiskers were symmetric. For Re2133/pKRSF1010-P_{j5}-egfp, the distribution range started to increase at 5 cell generations. On the last sample, the distribution could not be considered Gaussian anymore; a non-fluorescent subpopulation appeared and increased during the last hours of culture.

Cell permeabilization and eGFP excretion

For Re2133/pKRSF1010-Pl_{ac}-egfp, the percentage of permeabilized cells remained low, under 2% (Fig. 3c). However, this

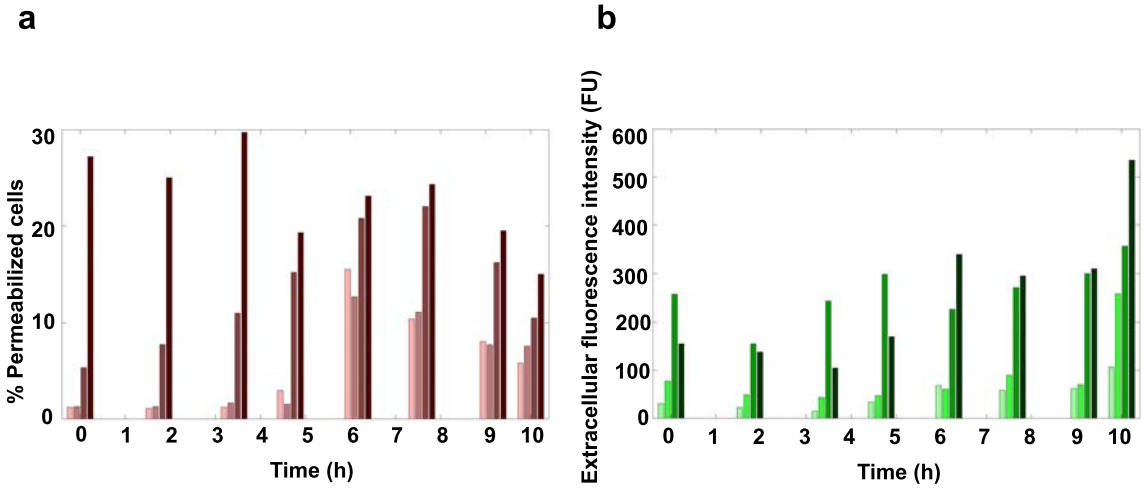

Fig. 2 **a** Percentage of permeabilized cells from broth cultures of *Cupriavidus necator* Re2133 strains during growth in flasks, harboring plasmids encoding for eGFP production with different constitutive promoters: Re2133/pKRSF1010-P_{j5}-eGFP ( ), Re2133/pKRSF1010-P_{n25}-eGFP ( ), Re2133/pKRSF1010-P_{tac}-eGFP ( ), and Re2133/pKRSF1010-P_{lac}-eGFP ( ). Data obtained by propidium iodide staining and flow cytometry (FL3 channel). **b** Extracellular fluorescence intensity from broth cultures of *Cupriavidus necator* Re2133 strains, harboring plasmids encoding for eGFP production with different constitutive: Re2133/pKRSF1010-P_{j5}-eGFP ( ), Re2133/pKRSF1010-P_{n25}-eGFP ( ), Re2133/pKRSF1010-P_{tac}-eGFP ( ), and Re2133/pKRSF1010-P_{lac}-eGFP ( ). Data obtained from fluorescence intensity measurements performed by a multiplate reader on broth sample supernatants

percentage increased all along the culture for Re2133/pKRSF1010-P_{j5}-egfp (Fig. 3d) and eventually reached 23% of permeabilized cells at 51 h.

Even if the extracellular fluorescence intensity increased for both strains, the levels reached by pKRSF1010-P_{j5}-egfp were 14-fold higher than those reached by pKRSF1010-P_{lac}-

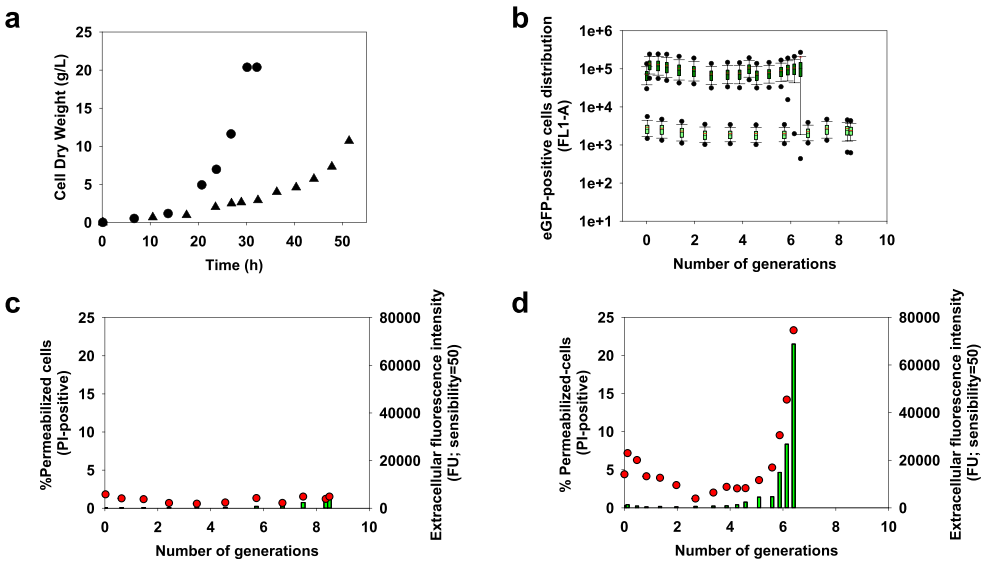

Fig. 3 **a** Growth kinetic in batch bioreactor of *Cupriavidus necator* Re2133 strains, harboring plasmids encoding for eGFP production with different constitutive promoters: Re2133/pKRSF1010-P_{lac}-eGFP (black-filled circle) and pKRSF1010-P_{j5}-eGFP (black-filled up-pointing triangle). Data obtained by optical density measurements at 600 nm. **b** Boxplot comparing the fluorescence intensity distribution depending on the cell generation number during batch bioreactor fermentations of the strains Re2133/pKRSF1010-P_{lac}-egfp ( ) and pKRSF1010-P_{j5}-egfp ( ). Data obtained by flow cytometry in FL1 channel. **c** Percentage of PI-positive cells ( ) and extracellular fluorescence intensity ( ), depending on the cell generation number, from batch cultures of *Cupriavidus necator* Re2133/pKRSF1010-P_{lac}-eGFP. Data obtained by flow cytometry (FL3 channel) and fluorescence measurements by a multiplate reader on supernatants. **d** Percentage of PI-positive cells ( ) and extracellular fluorescence intensity ( ), depending on the cell generation number, from batch cultures of *Cupriavidus necator* Re2133/pKRSF1010-P_{j5}-eGFP. Data obtained by flow cytometry (FL3 channel) and fluorescence measurements by a multiplate reader on supernatants

egfp, with a twofold lower biomass concentration.

Plasmid monitoring during batch culture: confrontation of fluorescence measurements with the traditional plate count method

To verify the validity of our plasmid expression level monitoring method, we confirmed our results with our reference method: parallel plate count.

For Re2133/pKRSF1010-P_{lac}-egfp, the results given by flow cytometry and plate count were comparable (Fig. 4a, c). The concentrations of eGFP-positive and gentamycin + kanamycin-resistant cells presented the same order of magnitude and the same evolution through time. The same observation can be made with the whole cell population and the gentamycin-resistant population concentration.

For Re2133/pKRSF1010-P_{j5}-egfp (Fig. 4b, d), cell concentrations given by plate count and flow cytometry seemed to evolve following the same dynamics. However, in the case of total cells and plasmid-bearing cell concentration, plate count gave lower results than fluorescence measurements all along the culture. So, plate count results were underestimated probably due to cultivability issues.

Fluorescence-activated cell sorting in conditions of plasmid curing by temperature

From the previous experiments, P_{lac} was chosen as the constitutive promoter to induce eGFP expression for the design of the plasmid expression level monitoring method; it was a good compromise between minimizing metabolic load on host cells and ensuring significant fluorescence intensity of single cells. So, the fluorescent cassette P_{lac}-egfp was cloned on a pBBad plasmid, and this backbone was used to encode recombinant molecule production (e.g., isopropanol (Crepin et al. 2016; Grousseau et al. 2014; Marc et al. 2017)) in our research team.

Our expression monitoring method was subjected to population heterogeneity in order to ensure that our eGFP biosensor would allow detecting it. So, the easiest approach was to induce population heterogeneity artificially. Plasmid-curing methods (Buckner et al. 2018; di Mauro et al. 1969; Trevors 1986) were reported in the literature to induce plasmid loss and population heterogeneity. In the present study, a plasmid-curing method based on temperature increase was set up to show the evolution of eGFP fluorescence intensity distribution within single cells in conditions of population heterogeneity. This experiment was based on successive subcultures of

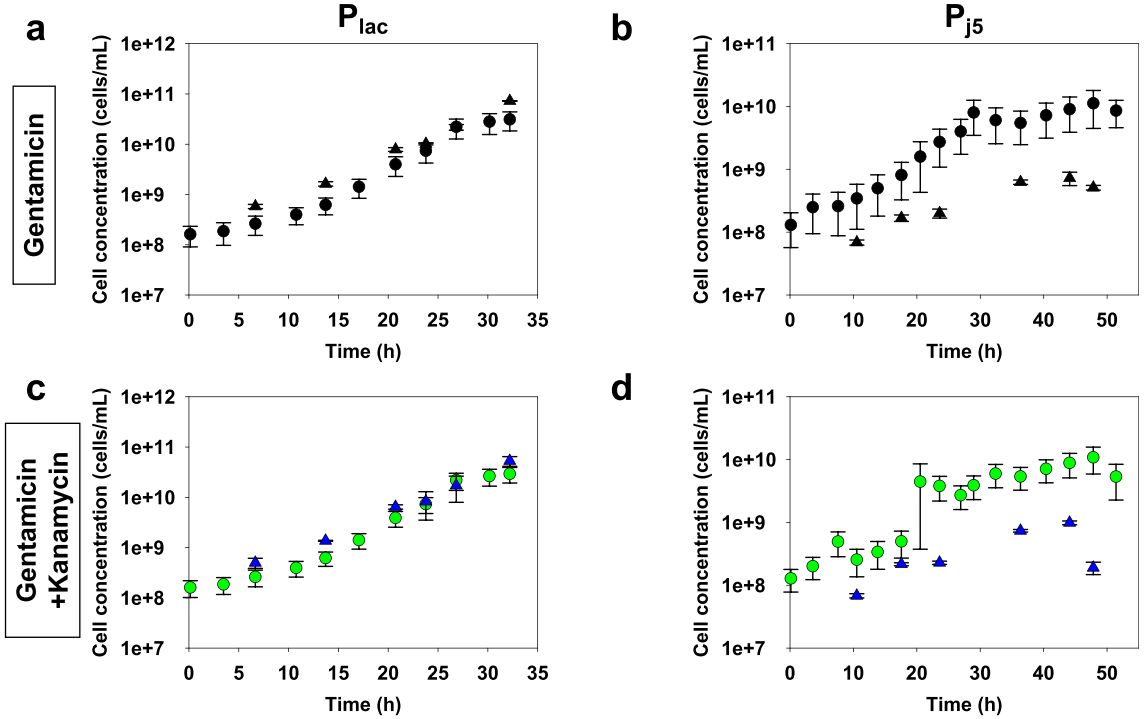

Fig. 4 **a** Comparison of the whole cell population concentration measured by flow cytometry (black-filled circle) and by plate count (black-filled up-pointing triangle) for Re2133/pKRSF1010-P_{lac}-eGFP during batch cultures. **b** Comparison of the amount of fluorescent cell concentration (green-filled circle) and the amount of kanamycin resistant cell concentration (blue-filled up-pointing triangle) for Re2133/pKRSF1010-P_{lac}-eGFP during batch cultures. **c** Comparison of the whole cell population concentration measured by flow cytometry (black-filled circle) and by plate count (black-filled up-pointing triangle) for Re2133/pKRSF1010-P_{j5}-eGFP during batch cultures. **d** Comparison of the amount of fluorescent cell concentration (green-filled circle) and the amount of kanamycin-resistant cell concentration (blue-filled up-pointing triangle) for Re2133/pKRSF1010-P_{j5}-eGFP during batch cultures

Re2133/pCB1 at 37 °C to maximize the number of cell generations exposed to plasmid-curing conditions.

Intensity fluorescence distribution during subcultures

After 6 successive subcultures (corresponding to 19 cell generations), only one subpopulation was observed. The fluorescence intensity distribution of eGFP-positive cells remained around a median of 3.6×10^3 in FL1-A, corresponding to the reference value for this strain under optimum culture conditions. The related population (2.1×10^3; 9.9×10^3) in the FL1-A channel was called "subpopulation P_2" (Fig. 5a). However, starting from 19 cell generations, three distinct subpopulations could be detected. Subpopulation P_2 remained visible. Another fluorescent subpopulation with a lower median value of 1.2×10^3 in FL1-A emerged; this corresponding population (4.9×10^2; 2.1×10^3) in the FL1-A channel was called "subpopulation P_1." A non-fluorescent subpopulation with a median of 2×10^2 in FL1-A appeared too; this related population (4.0×10^1; 4.9×10^2) in the FL1-A channel was named "subpopulation P_0."

Fluorescence-activated cell sorting was used to separate cells isolated from these three subpopulations according to their fluorescence intensity. The aim was to compare growth and fluorescent characteristics of the three subpopulations to better understand the loss of fluorescence intensity.

Cultivability and growth kinetics

During fluorescence-activated cell sorting (FACS), a single cell was deposited in each well of a 96-well plate. Six conditions were tested: subpopulations P_0, P_1, and P_2 were cultivated on TSB with 5 mg·L^{-1} gentamicin (total *C. necator* cells) and with 5 mg·L^{-1} gentamicin and 50 mg·L^{-1} kanamycin as a selection pressure (*C. necator* plasmid–bearing cells). The same antibiotic conditions were tested on solid medium for the subpopulations P_0, P_1, and P_2. All plates were incubated at 30 °C and multiplate reader measurements were performed regularly during cell growth on plates containing liquid medium.

No growth was detected for the population P_0, neither by absorbance measurements nor by fluorescence intensity measurements. Two hypotheses could explain this phenomenon: either cells or events were not cultivable or no cell was added to the plate because of too stringent selection conditions during cell sorting. The target criteria for cell selection before sorting based on fluorescence intensity were the same for all three subpopulations regarding the size (FSC) and the granulometry (SSC) of the cells. So, the absence of growth cannot be explained by a failure in the well inoculation.

However, cells grew on the plates containing subpopulations P_1 and P_2. On the plates containing subpopulation P_1 with gentamicin, growth was observed in 83% of the wells on liquid and 65% of the wells on solid medium. On the plates containing subpopulation P_1 with gentamicin + kanamycin, 80% of the wells on liquid and 70% of the wells on solid medium have grown. So, cells from the subpopulation P_1 were still resistant to kanamycin, as the percentages of growth were similar with and without selection pressure. On the plates containing subpopulation P_2 with gentamicin, 74% of the wells on liquid and 53% of the wells on solid medium presented growth. On the plates containing subpopulation P_2 with gentamicin + kanamycin, 71% of the wells on liquid and 58% of the wells on solid medium presented growth. So, cultivability was higher for the P_1 subpopulation compared with the P_2 subpopulation, both on liquid and on solid medium. For both subpopulations, cultivability was higher on liquid medium than on solid medium.

The mean growth rate was calculated for every well (Fig. 5b). On the one hand, P_1 cells tended to grow faster on average both on gentamicin at 0.07 ± 0.02 h^{-1} and on gentamicin + kanamycin at 0.09 ± 0.03 h^{-1}. On the other hand, P_2 cells grew slightly slower on average at 0.05 ± 0.01 h^{-1} on both antibiotic conditions.

Endpoint measurements of fluorescence intensity distribution in cell populations grown from single cells

In order to evaluate the fluorescent behavior of the progenies from the specific cell-sorted subpopulations (P_0, P_1, and P_2), the endpoint for each well was also analyzed by flow cytometry. Fluorescence intensity distribution regarding P_0, P_1, and P_2 subpopulations was determined based on the gates previously described (Fig. 5a). 3D scatter plots (Fig. 5c) were drawn in order to highlight sample variability according to the repartition of percentage of each subpopulation within a sample (i.e., well). The (x, y, z) coordinates of a point correspond to the percentage of fluorescent cells in P_0, P_1, or P_2 gates.

Three distinct clusters were identified and reported on 3D scatter plots. Thresholds of the red cluster (P_0 [0–10%]; P_1 [0–10%]; P_2 [80–100%]) corresponded to distributions composed of the highest P_2 cell contents. Thresholds of the purple cluster (P_0 [10–40%]; P_1 [25–35%]; P_2 [40–70%]) corresponded to distributions composed of the highest P_1 cell contents. The thresholds of the blue cluster (P_0 [10–40%]; P_1 [10–20%]; P_2 [40–70%]) corresponded to an intermediate cluster between the red and blue clusters.

According to each 3D scatter plot, one can clearly observe higher heterogeneity in the P_1 subpopulation progeny samples, in terms of endpoint fluorescence intensity distribution, compared with the subpopulation P_2 in both antibiotic conditions. Nevertheless, there was less heterogeneity for both subpopulations in the double antibiotic condition, which was more stringent.

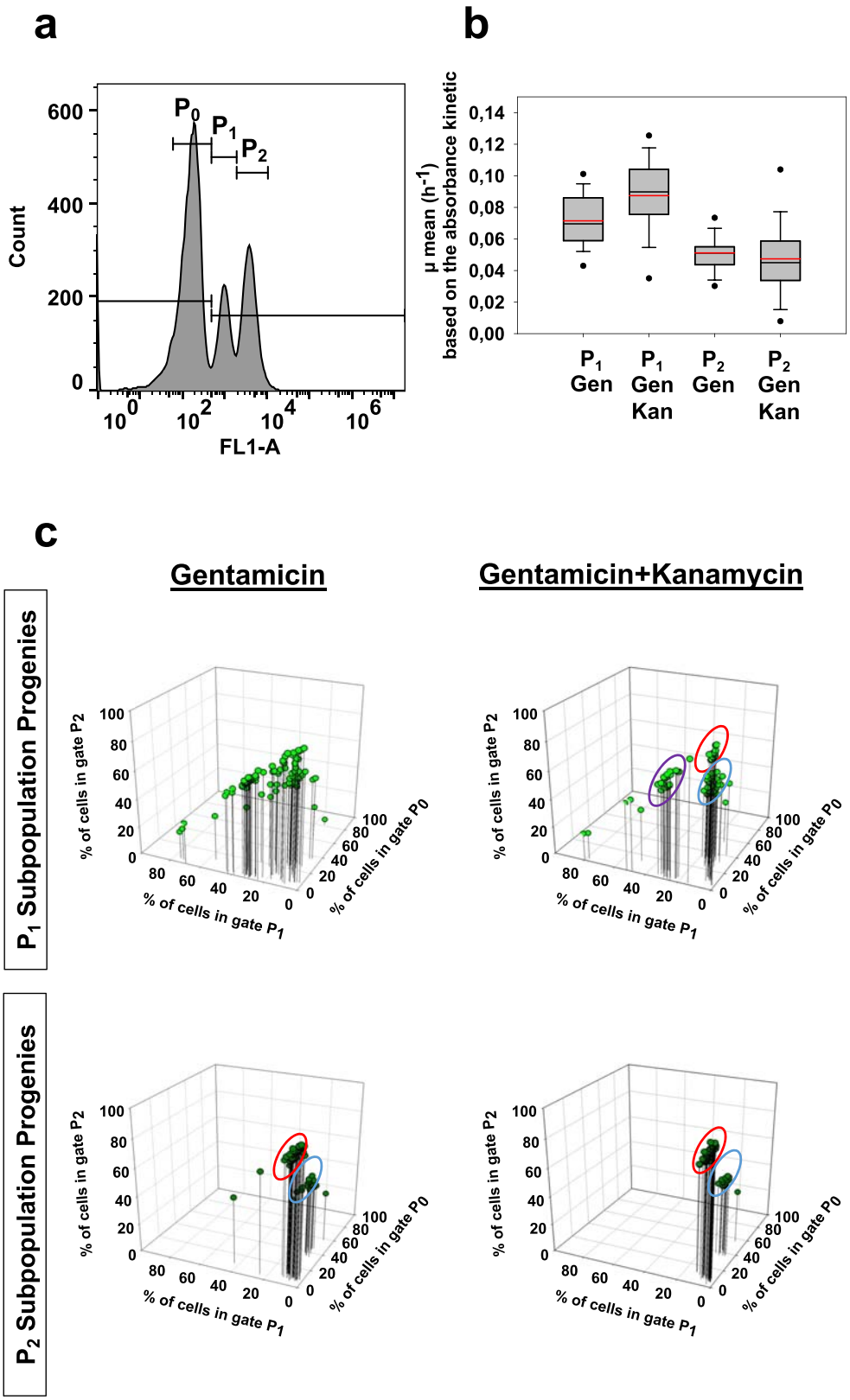

Fig. 5 **a** Fluorescence intensity distribution of the three subpopulations (P_0, P_1, and P_2) of *Cupriavidus necator* Re2133/pCB1 under plasmid-curing conditions. Data obtained by flow cytometry in channel FL1. **b** Boxplot comparing growth rates on the 96-well plates for the subpopulations P_1 and P_2, both on gentamicin and on gentamicin + kanamycin. Data obtained from optical density measurements at 600 nm. **c** Upper left: 3D scatter plot for fluorescence intensity distribution in the gates P_0, P_1, and P_2 for every well grown from a single cell from the subpopulation P_1 on gentamicin. Upper right: 3D scatter plot for fluorescence intensity distribution in the gates P_0, P_1, and P_2 for every well grown from a single cell from the subpopulation P_1 on gentamicin + kanamycin. Lower left: 3D scatter plot for fluorescence intensity distribution in the gates P_0, P_1, and P_2 for every well grown from a single cell from the subpopulation P_2 on gentamicin. Lower right: 3D scatter plot for fluorescence intensity distribution in the gates P_0, P_1, and P_2 for every well grown from a single cell from the subpopulation P_2 on gentamicin + kanamycin

The progenies of the cell-sorted subpopulation P_1, on selective medium, gave fluorescence distribution endpoints mostly composed of P_2 cells, like those shown in the blue (45% of sample distributions) and red (20% of sample distributions) clusters. However, the amount of P_1 cells in their fluorescence intensity distribution was the highest reached, like that shown by the purple cluster (25% of sample distributions).

Cells grown from the subpopulation P_2 on both antibiotic conditions gave fluorescence distribution endpoints mostly composed of P_2 cells, like those shown in the blue (30% of sample distributions) and red (70% of sample distributions) clusters.

Discussion

The goal of this study was to develop a quick and reliable method for monitoring variations in the constitutive expression level of reporter protein under dynamic bioprocesses. Because this technique was based on the expression of a recombinant eGFP by plasmid-bearing cells, a reporter system had to be chosen with the minimum impact on the physiology of host cells while allowing detectable cell fluorescence. As amply demonstrated in the literature (Bentley et al. 1990; De Gelder et al. 2007; Glick 1995; Million-Weaver and Camps 2014; Silva et al. 2012), the expression of a recombinant plasmid forces a metabolic burden on the host. In those publications, metabolic burden was quantified at the whole population scale by expression of plasmid-borne products, by the plasmid copy number in cells, and by plate count on selective medium. In the present study, the relative importance of the metabolic burden was evaluated indirectly from growth kinetics and cell physiology based on single-cell analyses in order to get access to the subpopulation distributions.

Flow cytometry had already been used to monitor plasmid stability within a pure culture of fluorescent *E. coli* strain in the work of Bahl et al. (2004). GFP expression was induced by a lac-promoter and encoded on the chromosome of *E. coli*. A functional *lacI* gene, encoding for a repressor protein, was integrated on the recombinant plasmid, thus preventing GFP expression initiation when plasmid is present in the cell. Inversely, GFP biosynthesis is induced after plasmid loss and plasmid-free cells were fluorescent. Our methods might be seen as complementary because of the two aims to detect expression heterogeneities: on the one hand, GFP production was a reporter for plasmid loss in Bahl et al. and on the other hand, eGFP production was a biosensor of plasmid expression level stability in our work. The accuracy of both methods was confronted to traditional plate count measurements. As for all biosensor-based approaches, bias has to be considered for both methods: (i) Half-life time of the molecules involved (i.e., eGFP and LacI) may lead to an underestimation of population heterogeneity; (ii) metabolic burden put on the host by the recombinant plasmid and/or the chromosomal insertion needs to be considered carefully in order to prevent phenotypic instability; metabolic burden might be the cause of plasmid instability or methylation of recombinant gene on the host's chromosome (Heller et al. 1995). Biosensors are precious tools for in vivo and/or in situ monitoring; however, it is crucial to be aware of the drawbacks.

In the work of Gruber et al. (2014), promoter strength has been evaluated at the whole population scale in the plasmids pKRSF1010/P_{lac}-egfp, pKRSF1010/P_{tac}-egfp, pKRSF1010/P_{n25}-egfp, and pKRSF1010/P_{j5}-egfp. The ranking of these promoters from the weakest to the strongest was P_{lac}, P_{tac}, P_{n25}, to P_{j5}. At the whole population level, the increase in fluorescence intensity was equal to 23% between P_{lac} and P_{tac}, 133% between P_{tac} and P_{n25}, and 100% between P_{n25} and P_{j5}. At the single-cell level, the ranking of these promoters according to their strength was confirmed; however, the increase in fluorescence intensity between promoters was more important when evaluated at the whole population level than at the single-cell level. Furthermore, for strong promoters like P_{j5}, the increase in the fluorescence intensity compared with medium strength promoters like P_{n25} was not as high as expected; over a critical threshold, there was no significant difference between medium and strong promoters at the single-cell level. This all suggested that the eGFP intensity measured at the whole population level might not entirely be due to intracellular eGFP. Most likely, eGFP molecules might be leaking outside the cells. This was confirmed by the fact that with increasing promoter strength, the percentage of permeabilized cells raised faster and higher, leading to higher eGFP excretion levels and lower fluorescence intensity of single cells. In that sense, after 5 cell generations in batch, the strain Re2133/pKRSF1010-P_{j5}-egfp presented a strong fluorescence intensity loss due to high permeabilization percentage and a high extracellular fluorescence. Promoter evaluation is usually done based on total fluorescence absorbance measurements using a spectrophotometer and a multiplate reader; this work demonstrates that an analysis at the single-cell level brings new insight into promoter evaluation.

The major effect in enhancing the promoter force was observed on growth kinetics, specifically through a decrease in the host maximal growth rate. For weak promoters as P_{lac} and P_{tac}, growth kinetic reduction was less drastic than for medium and strong promoters, P_{n25} and P_{j5}.

Furthermore, the results given by the two plasmid monitoring techniques were compared: parallel plate count and recombinant protein expression. By comparing these two methods, plasmid expression level stability was measured by detection of the expression of two different recombinant gene sets (eGFP and kanamycin resistance) encoded on the plasmid. For Re2133/pKRSF1010-P_{lac}-egfp cultures in batch, the two methods gave comparable results. However, for Re2133/

pKRSF1010-P_{j5}-egfp, plate count gave lower concentration than flow cytometry. This could be explained by the fact that plate counting depends on the cell's cultivability, which decreased drastically because of the metabolic load put on the host by P_{j5}. However, with both plate count and flow cytometry, no significant plasmid expression level fluctuations were observed during the tested culture conditions. To our knowledge, the drastic negative impact of the promoter P_{j5} on cell growth and physiology in the case of recombinant molecule production has never been highlighted before, and to our knowledge, indeed the very high strength of the constitutive promoter P_{j5} has always been presented as a positive productivity aspect like in the works of Gruber et al. (2014) and Lee et al. (2019), regarding eGFP and isoprene production, respectively. The use of stronger promoters leads to increased recombinant molecule production and so higher plasmid-related metabolic load. This increased protein production level might become toxic for the cells, as shown in the case of red fluorescent protein (Shemiakina et al. 2012).

So, in the present case study, the promoter P_{lac} has been chosen to constitutively induce the production of eGFP by plasmid-bearing cells, due to its significant fluorescence at the single-cell level and its low metabolic load on host cell metabolism.

When working with reporter molecules, the half-life time of the reporter protein must be considered. In this work, the ex vivo half-life time of eGFP was determined at 36 h (data not shown). Evidence was found in the literature that *Cupriavidus necator* has a particular segregation mechanism responsible for proper segregation of polyhydroxyalkanoate (PHA) granules during cell division and ensured, under balanced conditions, equal distribution of granules between daughter cells (Slaninova et al. 2018). It would be worth considering that the same mechanism would apply to eGFP and that after plasmid loss or expression cessation in the host cell, eGFP molecules in the mother cell should be equally segregated in daughter cells during cell division (Huh and Paulsson 2011). So, in the case where the signal is not saturated, fluorescence intensity eGFP should decrease exponentially in plasmid-free cells from generations to generations. Depending on their growth rate, cells may be counted as non-fluorescent in less than three cell generations (Alhumaizi et al. 2006). In conclusion, the non-eGFP-producing fluorescent cell population would present lower fluorescence intensity than eGFP-producing fluorescent cell population and consequently would lead to a significant decrease in fluorescence intensity distribution median after a single generation.

The eGFP biosensor needed to be subjected to population heterogeneity induced by plasmid-curing methods, to verify its accuracy in stringent conditions. After cell sorting, cells originated from the P_1 subpopulation were able to grow on kanamycin selection pressure, meaning that even after successive subcultures at 37 °C, cells of the P_1 subpopulation kept their plasmid. Plus, it had been shown that cells originated from the P_1 subpopulation grew faster and had a better cultivability both on liquid and solid medium than cells originated from the P_2 subpopulation. The favored hypothesis coming from these observations was that the reduced fluorescence intensity of P_1 subpopulation might be due to a lower eGFP expression in the cells compared to the P_2 subpopulation; indeed, a decrease in metabolic burden favored an increased growth rate of cell populations.

Like expected, cells from the P_2 subpopulation gave P_2 daughter cells after growth from a single cell. However, for cells from the P_1 subpopulation, only a small portion of wells (< 4%) were composed of 100% cells in the P_1 gate. Even if 25% of the wells gave cell populations with more than 25% of cells in the P_1 gate, it seemed like daughter cells from the subpopulation P_1 regained the ability to fluoresce higher (in the P_2 gate) after growth at optimal temperature of 30 °C; indeed 20% of wells gave cell population with more than 80% of cells in the P_2 gate.

In conclusion, the gene encoding for eGFP expression was inserted into different strains in order to analyze the fluorescence emitted at the single-cell level. This method offers the clear advantage of measuring the fluorescence emitted by eGFP molecules within single cells, thus giving access to the heterogeneity distribution within cell populations, whereas techniques at the whole population scale only measure the mean fluorescence emitted by cell populations. In this approach for plasmid expression level monitoring, it is crucial to minimize the effects of metabolic load on host.

We showed that increased promoter strength led to increased fluorescence intensity at the single-cell level up to a max and had a significant negative impact on growth kinetics and cell permeability. The use of the promoter P_{j5} led to strong fluorescence intensity loss, increased cell permeability, and important cultivability issues. Among all the promoters tested, P_{lac} presented with the lowest metabolic load on the host and ensured sufficient and significant fluorescence intensity of single cells; its use to control *egfp* transcription was found to be a good compromise. Batch cultivations showed that plasmid expression level monitoring by eGFP fluorescence measurement was a time-saving and relevant method, compared with the more traditional method of plate counting, when the weakest promoter P_{lac} was used. Plasmid-curing experiments on the strain Re2133/pCB1 showed the apparition of three subpopulations of P_0, P_1, and P_2 characterized by different fluorescence intensities at the single-cell level. The subpopulation P_0 was the non-fluorescent population

and the subpopulation P_2 was the reference fluorescent population. The decreased fluorescence intensity of the subpopulation P_1 compared with the subpopulation P_2 was due to an adaptation of eGFP expression levels in single cells in response to thermal stress. For the population P_1, the decrease in eGFP expression level was correlated with a decrease in metabolic load and so increased growth rate and cultivability when cells grown again at 30 °C. So, our plasmid expression level reporter system based on an eGFP biosensor allowed detecting population heterogeneity in plasmid-curing-like conditions with different plasmid expression levels.

Further steps would be testing our expression monitoring technique under "toxic" recombinant molecule–producing conditions in order to better understand the causes of plasmid expression level heterogeneity.

Acknowledgments We thank Petra Heidinger for the generous gift of the pKRSF1010 plasmids and fruitful discussions. We thank Delphine Lestrade from TWB for her assistance and expertise during the cell sorting experiments.

Authors' contributions statement CB, JL, SA, NG, and SG conceived and designed research. CB conducted experiments and analyzed data. CB wrote the manuscript and JL, SA, NG, and SG reviewed it. All authors read and approved the manuscript.

Availability of data and material All data generated or analyzed during this study are included in the present work.
Code availability Not applicable.

Funding information Funding was obtained from Doctoral Research Assignments from the French Ministry of Research.

Compliance with ethical standards

Competing interests The authors declare that they have no competing interests.

Ethical approval Not applicable, since the work does not involve any study with human participants or animals.

Consent to participate Not applicable.

References

Alhumaizi K, Alwan A, Ajbar A (2006) Competition of plasmid-bearing and plasmid-free organisms in a chemostat: a study of bifurcation phenomena. Math Comput Model 44(3–4):342–367. https://doi.org/10.1016/j.mcm.2006.01.021

Bahl ML, Sorensen SJ, Hansen LH (2004) Quantification of plasmid loss in *Escherichia coli* cells by use of flow cytometry. FEMS Microbiol Lett 232(1):45–49. https://doi.org/10.1016/s0378-1097(04)00015-1

Bentley WE, Quiroga OE (1993) Investigation of subpopulation heterogeneity and plasmid stability in recombinant *Escherichia coli* via simple segregated model. Biotechnol Bioeng 42(2):222–234. https://doi.org/10.1002/bit.260420210

Bentley WE, Mirjalili N, Andersen DC, Davis RH, Kompala DS (1990) Plasmid-encoded protein: the principal factor in the "metabolic burden" associated with recombinant bacteria. Biotechnol Bioeng 35(7):668–681. https://doi.org/10.1002/bit.260350704

Bi CH, Su P, Muller J, Yeh YC, Chhabra SR, Beller HR, Singer SW, Hillson NJ (2013) Development of a broad-host synthetic biology toolbox for *Ralstonia eutropha* and its application to engineering hydrocarbon biofuel production. Microb Cell Factories 12:1–10. https://doi.org/10.1186/1475-2859-12-107

Binder D, Drepper T, Jaeger KE, Delvigne F, Wiechert W, Kohlheyer D, Grunberger A (2017) Homogenizing bacterial cell factories: analysis and engineering of phenotypic heterogeneity. Metab Eng 42:145–156. https://doi.org/10.1016/j.ymben.2017.06.009

Brehm-Stecher BF, Johnson EA (2004) Single-cell microbiology: tools, technologies, and applications. Microbiol Mol Biol R 68(3):538. https://doi.org/10.1128/mmbr.68.3.538-559.2004

Buckner MMC, Ciusa ML, Piddock LJV (2018) Strategies to combat antimicrobial resistance: anti-plasmid and plasmid curing. Fems Microbiol R 42(6):781–804. https://doi.org/10.1093/femsre/fuy031

Budde CF, Riedel SL, Willis LB, Rha C, Sinskey AJ (2011) Production of poly(3-hydroxybutyrate-co-3-hydroxyhexanoate) from plant oil by engineered *Ralstonia eutropha* strains. Appl Environ Microbiol 77(9):2847–2854. https://doi.org/10.1128/aem.02429-10

Carlquist M, Fernandes RL, Helmark S, Heins AL, Lundin L, Sorensen SJ, Gernaey KV, Lantz AE (2012) Physiological heterogeneities in microbial populations and implications for physical stress tolerance. Microb Cell Factories 11. https://doi.org/10.1186/1475-2859-11-94

Ceroni F, Boo A, Furini S, Gorochowski TE, Borkowski O, Ladak YN, Awan AR, Gilbert C, Stan GB, Ellis T (2018) Burden-driven feedback control of gene expression. Nat Methods 15(5):387. https://doi.org/10.1038/nmeth.4635

Cinelli RAG, Ferrari A, Pellegrini V, Tyagi M, Giacca M, Beltram F (2000) The enhanced green fluorescent protein as a tool for the analysis of protein dynamics and localization: local fluorescence study at the single-molecule level. Photochem Photobiol 71(6):771–776. https://doi.org/10.1562/0031-8655(2000)071<0771:tegfpa>2.0.co;2

Crepin L, Lombard E, Guillouet SE (2016) Metabolic engineering of *Cupriavidus necator* for heterotrophic and autotrophic alka(e)ne production. Metab Eng 37:92–101. https://doi.org/10.1016/j.ymben.2016.05.002

De Gelder L, Ponciano JM, Joyce P, Top EM (2007) Stability of a promiscuous plasmid in different hosts: no guarantee for a long-term relationship. Microbiol-Sgm 153:452–463. https://doi.org/10.1099/mic.0.2006/001784-0

Delvigne F, Goffin P (2014) Microbial heterogeneity affects bioprocess robustness: dynamic single-cell analysis contributes to understanding of microbial populations. Biotechnol J 9(1):61–72. https://doi.org/10.1002/biot.201300119

Elowitz MB, Levine AJ, Siggia ED, Swain PS (2002) Stochastic gene expression in a single cell. Science 297(5584):1183–1186. https://doi.org/10.1126/science.1070919

Ewering C, Heuser F, Benolken JK, Bramer C, Steinbuchel A (2006) Metabolic engineering of strains of *Ralstonia eutropha* and *Pseudomonas putida* for biotechnological production of 2-methylcitric acid. Metab Eng 8(6):587–602. https://doi.org/10.1016/j.ymben.2006.05.007

Friedrich CG, Bowien B, Friedrich B (1979) Formate and oxalate metabolism in *Alcaligenes eutrophus*. J Gen Microbiol 115(NOV):185–192. https://doi.org/10.1099/00221287-115-1-185

Fukui T, Suzuki M, Tsuge T, Nakamura S (2009) Microbial synthesis of poly((R)-3-hydroxybutyrate-co-3-hydroxypropionate) from unrelated carbon sources by engineered *Cupriavidus necator*. Biomacromolecules 10(4):700–706. https://doi.org/10.1021/bm801391j

Fukui T, Ohsawa K, Mifune J, Orita I, Nakamura S (2011) Evaluation of promoters for gene expression in polyhydroxyalkanoate-producing *Cupriavidus necator* H16. Appl Microbiol Biotechnol 89(5):1527–1536. https://doi.org/10.1007/s00253-011-3100-2

Glick BR (1995) Metabolic load and heterologous gene-expression. Biotechnol Adv 13(2):247–261. https://doi.org/10.1016/0734-9750(95)00004-a

Gonzalez-Cabaleiro R, Mitchell AM, Smith W, Wipat A, Ofiteru ID (2017) Heterogeneity in pure microbial systems: experimental measurements and modeling. Front Microbiol 8. https://doi.org/10.3389/fmicb.2017.01813

Grousseau E, Lu JN, Gorret N, Guillouet SE, Sinskey AJ (2014) Isopropanol production with engineered *Cupriavidus necator* as bioproduction platform. Appl Microbiol Biotechnol 98(9):4277–4290. https://doi.org/10.1007/s00253-014-5591-0

Gruber S, Hagen J, Schwab H, Koefinger P (2014) Versatile and stable vectors for efficient gene expression in *Ralstonia eutropha* H16. J Biotechnol 186:74–82. https://doi.org/10.1016/j.jbiotec.2014.06.030

Gruber S, Schwab H, Koefinger P (2015) Versatile plasmid-based expression systems for Gram-negative bacteria-general essentials exemplified with the bacterium *Ralstonia eutropha* H16. New Biotechnol 32(6):552–558. https://doi.org/10.1016/j.nbt.2015.03.015

Gruber S, Schwendenwein D, Magomedova Z, Thaler E, Hagen J, Schwab H, Heidinger P (2016) Design of inducible expression vectors for improved protein production in *Ralstonia eutropha* H16 derived host strains. J Biotechnol 235:92–99. https://doi.org/10.1016/j.jbiotec.2016.04.026

Grunwald S, Mottet A, Grousseau E, Plassmeier JK, Popovic MK, Uribelarrea JL, Gorret N, Guillouet SE, Sinskey A (2015) Kinetic and stoichiometric characterization of organoautotrophic growth of *Ralstonia eutropha* on formic acid in fed-batch and continuous cultures. Microb Biotechnol 8(1):155–163. https://doi.org/10.1111/1751-7915.12149

Haroon MF, Skennerton CT, Steen JA, Lachner N, Hugenholtz P, Tyson GW (2013) In-solution fluorescence in situ hybridization and fluorescence-activated cell sorting for single cell and population genome recovery. In: DeLong EF (ed) Microbial metagenomics, metatranscriptomics, and metaproteomics, Methods in enzymology, vol 531. Elsevier Academic Press Inc, San Diego, pp 3–19

Heller H, Kammer C, Wilgenbus P, Doerfler W (1995) Chromosomal insertion of foreign (Adenovirus-type-12, plasmid, or bacteriophage-lambda) DNA is associated with enhanced methylation of cellular DNA segments. Proc Natl Acad Sci USA 92(12):5515–5519. https://doi.org/10.1073/pnas.92.12.5515

Hoefel T, Wittmann E, Reinecke L, Weuster-Botz D (2010) Reaction engineering studies for the production of 2-hydroxyisobutyric acid with recombinant *Cupriavidus necator* H 16. Appl Microbiol Biotechnol 88(2):477–484. https://doi.org/10.1007/s00253-010-2739-4

Huh D, Paulsson J (2011) Random partitioning of molecules at cell division. Proc Natl Acad Sci USA 108(36):15004–15009. https://doi.org/10.1073/pnas.1013171108

Johnson BFRYS (1971) Dissimilation of aromatic compounds by *Alcaligenes eutrophus*. J Bacteriol 107(2):468–475

Lee CL, Ow DSW, Oh SKW (2006) Quantitative real-time polymerase chain reaction for determination of plasmid copy number in bacteria. J Microbiol Methods 65(2):258–267. https://doi.org/10.1016/j.mimet.2005.07.019

Lee HW, Park JH, Lee HS, Choi W, Seo SH, Anggraini ID, Choi ES, Lee HW (2019) Production of bio-based isoprene by the mevalonate pathway cassette in *Ralstonia eutropha*. J Microbiol Biotechnol 29(10):1656–1664. https://doi.org/10.4014/jmb.1909.09002

Loftie-Eaton W, Tucker A, Norton A, Top EM (2014) Flow cytometry and real-time quantitative PCR as tools for assessing plasmid persistence. Appl Environ Microbiol 80(17):5439–5446. https://doi.org/10.1128/aem.00793-14

Lu JN, Brigham CJ, Rha C, Sinskey AJ (2013) Characterization of an extracellular lipase and its chaperone from *Ralstonia eutropha* H16. Appl Microbiol Biotechnol 97(6):2443–2454. https://doi.org/10.1007/s00253-012-4115-z

Marc J, Grousseau E, Lombard E, Sinskey AJ, Gorret N, Guillouet SE (2017) Over expression of GroESL in *Cupriavidus necator* for heterotrophic and autotrophic isopropanol production. Metab Eng 42:74–84. https://doi.org/10.1016/j.ymben.2017.05.007

Martins BMC, Locke JOW (2015) Microbial individuality: how single-cell heterogeneity enables population level strategies. Curr Opin Microbiol 24:104–112. https://doi.org/10.1016/j.mib.2015.01.003

di Mauro E, Synder L, Marino P, Lamberti A, Coppo A, Tocchini-Valentini GP (1969) Rifampicin sensitivity of the components of DNA-dependent RNA polymerase. Nature 222(5193):533–537. https://doi.org/10.1038/222533a0

Mifune J, Nakamura S, Fukui T (2010) Engineering of pha operon on *Cupriavidus necator* chromosome for efficient biosynthesis of poly(3-hydroxybutyrate-co-3-hydroxyhexanoate) from vegetable oil. Poly Degrad Stabil 95(8):1305–1312. https://doi.org/10.1016/j.polymdegradstab.2010.02.026

Million-Weaver S, Camps M (2014) Mechanisms of plasmid segregation: have multicopy plasmids been overlooked? Plasmid 75:27–36. https://doi.org/10.1016/j.plasmid.2014.07.002

Mortier J, Tadesse W, Govers SK, Aertsen A (2019) Stress-induced protein aggregates shape population heterogeneity in bacteria. Curr Genet 65(4):865–869. https://doi.org/10.1007/s00294-019-00947-1

Muller S, Nebe-von-Caron G (2010) Functional single-cell analyses: flow cytometry and cell sorting of microbial populations and communities. Fems Microbiol R 34(4):554–587. https://doi.org/10.1111/j.1574-6976.2010.00214.x

Muller S, Harms H, Bley T (2010) Origin and analysis of microbial population heterogeneity in bioprocesses. Curr Opin Biotechnol 21(1):100–113. https://doi.org/10.1016/j.copbio.2010.01.002

Muller J, MacEachran D, Burd H, Sathitsuksanoh N, Bi CH, Yeh YC, Lee TS, Hillson NJ, Chhabra SR, Singer SW, Beller HR (2013) Engineering of *Ralstonia eutropha* H16 for autotrophic and heterotrophic production of methyl ketones. Appl Environ Microbiol 79(14):4433–4439. https://doi.org/10.1128/aem.00973-13

Nana GYG, Ripoll C, Cabin-Flaman A, Gibouin D, Delaune A, Janniere L, Grancher G, Chagny G, Loutelier-Bourhis C, Lentzen E, Grysan P, Audinot JN, Norris V (2018) Division-based, growth rate diversity in bacteria. Front Microbiol 9. https://doi.org/10.3389/fmicb.2018.00849

Rakotomalala R (2011) Tests de normalité - Techniques empiriques et tests statistiques. Université Lumière, Lyon, p 2

Sato S, Fujiki T, Matsumoto K (2013) Construction of a stable plasmid vector for industrial production of poly(3-hydroxybutyrate-co-3-hydroxyhexanoate) by a recombinant *Cupriavidus necator* H16 strain. J Biosci Bioeng 116(6):677–681. https://doi.org/10.1016/j.jbiosc.2013.05.026

Shaner NC, Steinbach PA, Tsien RY (2005) A guide to choosing fluorescent proteins. Nat Methods 2(12):905–909. https://doi.org/10.1038/nmeth819

Shemiakina II, Ermakova GV, Cranfill PJ, Baird MA, Evans RA, Souslova EA, Staroverov DB, Gorokhovatsky AY, Putintseva EV, Gorodnicheva TV, Chepurnykh TV, Strukova L, Lukyanov S, Zaraisky AG, Davidson MW, Chudakov DM, Shcherbo D (2012) A monomeric red fluorescent protein with low cytotoxicity. Nat Commun:3. https://doi.org/10.1038/ncomms2208

Silva F, Queiroz JA, Domingues FC (2012) Evaluating metabolic stress and plasmid stability in plasmid DNA production by *Escherichia coli*. Biotechnol Adv 30(3):691–708. https://doi.org/10.1016/j.biotechadv.2011.12.005

Skulj M, Okrslar V, Jalen S, Jevsevar S, Slanc P, Strukelj B, Menart V (2008) Improved determination of plasmid copy number using quantitative real-time PCR for monitoring fermentation processes. Microb Cell Factories:7. https://doi.org/10.1186/1475-2859-7-6

Slaninova E, Sedlacek P, Mravec F, Mullerova L, Samek O, Koller M, Hesko O, Kucera D, Marova I, Obruca S (2018) Light scattering on PHA granules protects bacterial cells against the harmful effects of UV radiation. Appl Microbiol Biotechnol 102(4):1923–1931. https://doi.org/10.1007/s00253-018-8760-8

Slater S, Houmiel KL, Tran M, Mitsky TA, Taylor NB, Padgette SR, Gruys KJ (1998) Multiple beta-ketothiolases mediate poly(beta-hydroxyalkanoate) copolymer synthesis in *Ralstonia eutropha*. J Bacteriol 180(8):1979–1987

Sydow A, Pannek A, Krieg T, Huth I, Guillouet SE, Holtmann D (2017) Expanding the genetic tool box for *Cupriavidus necator* by a stabilized L-rhamnose inducible plasmid system. J Biotechnol 263:1–10. https://doi.org/10.1016/j.jbiotec.2017.10.002

Tal S, Paulsson J (2012) Evaluating quantitative methods for measuring plasmid copy numbers in single cells. Plasmid 67(2):167–173. https://doi.org/10.1016/j.plasmid.2012.01.004

Tracy BP, Gaida SM, Papoutsakis ET (2010) Flow cytometry for bacteria: enabling metabolic engineering, synthetic biology and the elucidation of complex phenotypes. Curr Opin Biotechnol 21(1):85–99. https://doi.org/10.1016/j.copbio.2010.02.008

Trevors JT (1986) Plasmid curing in bacteria. FEMS Microbiol Lett 32(3–4):149–157

Wegrzyn G, Wegrzyn A (2002) Stress responses and replication of plasmids in bacterial cells. Microb Cell Factories 1. https://doi.org/10.1186/1475-2859-1-2

Wong YM, Brigham CJ, Rha C, Sinskey AJ, Sudesh K (2012) Biosynthesis and characterization of polyhydroxyalkanoate containing high 3-hydroxyhexanoate monomer fraction from crude palm kernel oil by recombinant *Cupriavidus necator*. Bioresour Technol 121:320–327. https://doi.org/10.1016/j.biortech.2012.07.015

Zielenkiewicz U, Ceglowski P (2001) Mechanisms of plasmid stable maintenance with special focus on plasmid addiction systems. Acta Biochim Pol 48(4):1003–1023

Publisher's note Springer Nature remains neutral with regard to jurisdictional claims in published maps and institutional affiliations.